Steroids 96 (2015) 63–72

Contents lists available at ScienceDirect

Steroids

journal homepage: www.elsevier.com/locate/steroids

Calotroposides H–N, new cytotoxic oxypregnane oligoglycosides from the root bark of *Calotropis procera*

Sabrin R.M. Ibrahim [a,b], Gamal A. Mohamed [c,d], Lamiaa A. Shaala [e,f], Laetitia Moreno Y. Banuls [g], Robert Kiss [g], Diaa T.A. Youssef [c,h,*]

[a] Department of Pharmacognosy and Pharmaceutical Chemistry, Faculty of Pharmacy, Taibah University, Al Madinah Al Munawarah 30078, Saudi Arabia
[b] Department of Pharmacognosy, Faculty of Pharmacy, Assiut University, Assiut 71526, Egypt
[c] Department of Natural Products, Faculty of Pharmacy, King Abdulaziz University, Jeddah 21589, Saudi Arabia
[d] Department of Pharmacognosy, Faculty of Pharmacy, Al-Azhar University, Assiut Branch, Assiut 71524, Egypt
[e] Natural Products Unit, King Fahd Medical Research Center, King Abdulaziz University, Jeddah 21589, Saudi Arabia
[f] Suez Canal University Hospital, Suez Canal University, Ismailia 41522, Egypt
[g] Laboratoire de Cancérologie et de Toxicologie Expérimentale, Faculté de Pharmacie, Université Libre de Bruxelles, Bruxelles, Belgium
[h] Department of Pharmacognosy, Faculty of Pharmacy, Suez Canal University, Ismailia 41522, Egypt

ARTICLE INFO

Article history:
Received 6 September 2014
Received in revised form 16 December 2014
Accepted 14 January 2015
Available online 30 January 2015

Keywords:
Asclepiadaceae
Calotropis procera
Oxypregnane
Calotroposides H–N
Cancer growth inhibitory activity

ABSTRACT

As a part of our continuing interest in identifying anticancer drug leads from natural sources, we have investigated the *n*-BuOH fraction of the root bark of *Calotropis procera* (Ait) R. Br. Seven new oxypregnane oligoglycosides: calotroposides H–N (**1–7**) were isolated and identified. Their structures were established on the basis of 1D and 2D NMR studies, HRMS, and GCMS spectral data. The *in vitro* growth inhibitory activity of the *n*-BuOH fraction and compounds **1–7** was evaluated against A549 non-small cell lung cancer (NSCLC), U373 glioblastoma (GBM), and PC-3 prostate cancer cell lines. Compounds **4** and **6** showed subnanomolar growth inhibition activity with IC_{50} ranging from 0.5 to 0.7 μM against U373 glioblastoma (GBM) and PC-3 prostate cancer cell lines. These results provide further insight into the chemical diversity and biological activities of this class of compounds.

1. Introduction

Asclepiadaceae family comprises about 175–180 genera and 2200 species distributed in the tropical and subtropical regions [1]. *Calotropis* is a small genus having 6 species of shrubs or small trees, distributed in tropical and subtropical Africa, Asia, and America [1]. *Calotropis procera* is a wild-growing tropical plant, known by various names like dead sea apple, swallow wort, and milk weed. It is commonly used in the traditional treatment of epilepsy, inflammation, microbial and protozoan infections [2,3]. The plant possesses different biological activities including: anti-inflammatory, analgesic, antitumor, anti-diarrheal, hepatoprotective, antiulcer, anthelmintic, insecticidal, antioxidant, antibacterial, and spasmolytic [4–10]. We have identified a novel cardenolide, 2″-oxovoruscharin, in *C. procera* samples growing in Burkina Faso from which we hemisynthesized 19-hydroxy-2″-oxovoruscharin [6]. Our previous phytochemical study of the *n*-hexane fraction of *C. procera* root bark from Egypt led to the isolation of ursane-type triterpenes and cardiac glycoside [11,12]. In a continuation of our interest to search for drug leads from natural sources, we have investigated the *n*-BuOH fraction of the root bark of *C. procera* growing in Egypt. Bioassay-directed fractionation of the active *n*-BuOH fraction using A549 NSCLC, U373 GBM, and PC-3 prostate cancer cell lines led to the isolation of seven new oxypregnane oligoglycosides: calotroposides H–N (**1–7**) (Fig. 1). Their structures were verified by various spectroscopic methods. The isolated compounds were evaluated for their *in vitro* growth inhibitory activity using the MTT colorimetric assay.

2. Experimental

2.1. General experimental procedures

Optical rotations were measured on a Perkin–Elmer Model 341 LC polarimeter (Perkin–Elmer, Waltham, MA, USA). IR spectra were measured with a Shimadzu Infrared-400 spectrophotometer (Shimadzu, Kyoto, Japan). The UV spectra were carried out in

* Corresponding author at: Department of Natural Products, Faculty of Pharmacy, King Abdulaziz University, Jeddah 21589, Saudi Arabia. Tel.: +966 548 535 344; fax: +966 269 516 96.
E-mail address: dyoussef@kau.edu.sa (D.T.A. Youssef).

http://dx.doi.org/10.1016/j.steroids.2015.01.012
0039-128X/

MeOH using a Perkin-Elmer Lambda 25 UV/VIS spectrophotometer (Perkin–Elmer, Waltham, MA, USA). ESIMS spectra were recorded on a Finnigan MAT TSQ-7000 triple stage quadrupole mass spectrometer (ThermoFinnigan, Bremen, Germany). HRESIMS spectra were obtained using an LTQ Orbitrap mass spectrometer (Thermo Fisher, Waltham, MA, USA). A GCMS was performed on Clarus 500 GC/MS (Perkin–Elmer, Waltham, MA, USA). The software controller/integrator was turbo mass, version 4.5.0.007 (Perkin–Elmer, Waltham, MA, USA). An elite 5 MS GC capillary column (30 × 0.25 mm × 0.5 μm, Perkin–Elmer, Waltham, MA, USA) was used. The carrier gas was helium at a flow rate of 2 mL/min (32 p.s.i., flow initial 55.8 cm/s, split; 1:40). Temperature conditions were: inlet line temperature, 200 °C; source temperature, 150 °C; trap emission, 100 °C; and electron energy, 70 eV. The column temperature program was: 50 °C for 5 min, increased to 220 °C (rate, 20 °C/min), and held for 5 min. The injector temperature was 220 °C. MS scan was from 50 to 650 *m/z*. ^{1}H and ^{13}C NMR spectra were measured on a Bruker DRX 400 and 600 spectrometers (Bruker, Rheinstetten, Germany). 1D NMR spectral data were measured at a temperature of 23.7 °C and 2D NMR (^{1}H–^{1}H COSY, multiplicity-edited HSQC, and HMBC) spectral data were measured at a temperature of 26.85 °C. HPLC purification was performed on a semi-preparative HPLC system consisting of a Lachrom–Merck Hitachi L-7100 pump and a L-7400 UV detector using a C-18 column (300 × 8 mm i.d., prefilled with Eurospher 100, (Knauer, Berlin, Germany), with a flow rate of 5.0 mL/min, in an isocratic elution condition. The effluents were monitored by the DAD detector at 220 nm. Vacuum liquid chromatography (VLC) was performed using silica gel 60 (0.04–0.063 mm, Merck, Darmstadt, Germany). Column chromatographic separations were performed on silica gel 60 (0.04–0.063 mm, Merck, Darmstadt, Germany), RP-18 (0.04–0.063 mm, Merck, Darmstadt, Germany), and Sephadex LH-20 (0.25–0.1 mm, Merck, Darmstadt, Germany). TLC analyses were conducted on pre-coated silica gel F_{254} aluminum sheets (Merck, Darmstadt, Germany). Compounds were detected by spraying the sheets with *p*-anisaldehyde/H_2SO_4 reagent followed by heating at 110 °C for 1–2 min. Authentic sugars samples were purchased from Haihang Industry Co., Ltd. (South Gongye Rd, Jinan City, China).

2.2. Plant material

The root barks of *C. procera* were collected in April 2009 from trees growing in Ismailia, Egypt. The plant material was kindly identified by Prof. Dr. A. Fayed (Professor of Plant Taxonomy, Faculty of Science, Assiut University, Assiut, Egypt). A voucher specimen was deposited at the Herbarium of Pharmacognosy Department, Faculty of Pharmacy, Suez Canal University, Ismailia, Egypt (Registration code DY-CP-2009).

2.3. Extraction and isolation

The air-dried powdered root bark (1.2 kg) was extracted with MeOH (3.5 L × 4) at room temperature. The combined extracts were concentrated under reduced pressure to afford a dark brownish residue (55.0 g). The latter was suspended in distilled water (400 mL) followed by successive extraction with *n*-hexane (400 mL × 4), $CHCl_3$ (400 mL × 4), EtOAc (400 mL × 4), and *n*-BuOH (400 mL × 3). Each fraction was concentrated under reduced pressure to give *n*-hexane (4.5 g), $CHCl_3$ (3.2 g), EtOAc (5.6 g), and *n*-BuOH (7.5 g) fractions. The anticancer *n*-BuOH fraction was subjected to VLC using $CHCl_3$/MeOH gradient and collected fractions were grouped to obtain 4 major subfractions: A (1.6 g), B (1.9 g), C (1.8 g), and D (2.1 g). Fraction B (1.9 g) was subjected to SiO_2 column (150 g × 50 cm × 5 cm) and eluted with $CHCl_3$/MeOH gradient. Fractions 50 mL each were collected and monitored with TLC then similar fractions were grouped together. The fractions eluted with $CHCl_3$/MeOH (85/15) was subjected to RP-18 column (100 g × 50 cm × 3 cm) using MeOH/H_2O gradient elution to give impure compounds **1** and **2** which were further purified by HPLC (YMC-ODS-AQ, 250 × 20 mm) using CH_3CN/H_2O (25:75 → 45:55) to afford compounds **1** (15 mg) and **2** (18 mg). Sephadex LH-20 column chromatography of fraction C (1.8 g) using MeOH as an eluent afforded two major subfractions: C-1 (550 mg) and C-2 (1.1 g). Fraction C-2 was purified on HPLC (YMC-ODS-AQ, 250 × 20 mm) using CH_3CN/H_2O (25:75 → 50:50) to give compounds **3** (17 mg), **4** (19 mg), and **5** (13 mg). Fraction D (2.1 g) was chromatographed over a SiO_2 column (150 g × 50 cm × 5 cm) using a $CHCl_3$/MeOH gradient to give two major subfractions: D-1 (940 mg) and D-2 (560 mg). Subfraction D-1 was purified on HPLC (YMC-ODS-AQ, 250 × 20 mm) using CH_3CN/H_2O (25:75 → 50:50) to afford compound **6** (14 mg). Subfraction D-2 was subjected to Sephadex LH-20 column using MeOH as an eluent to afford impure **7**, which further purified on HPLC (YMC-ODS-AQ, 250 × 20 mm) using CH_3CN/H_2O to obtain compound **7** (16 mg).

2.3.1. Calotroposide H (**1**)

Brown viscous residue; $[\alpha]_D$ + 2.8 (*c* 1.1, MeOH); UV (MeOH) λ_{max} (log ε): 215 (4.23), 225 (4.11), 278 (3.28) nm; IR (KBr) ν_{max}: 3435, 2940, 1714, 1055 cm^{-1}; NMR data, see Tables 1–4; HRESIMS *m/z*: 1189.6519 $[M+H]^+$ (calcd for $C_{63}H_{97}O_{21}$, 1189.6522), 1211.6348 $[M+Na]^+$ (calcd for $C_{63}H_{96}O_{21}Na$, 1211.6342).

2.3.2. Calotroposide I (**2**)

Brown viscous residue; $[\alpha]_D$ + 18.1 (*c* 1.1, MeOH); UV (MeOH) λ_{max} (log ε): 215 (4.23), 225 (4.11), 278 (3.28) nm; IR (KBr) ν_{max}: 3465, 2943, 1710, 1455, 1065 cm^{-1}; NMR data, see Tables 1–4; HRESIMS *m/z*: 1189.6524 $[M+H]^+$ (calcd for $C_{63}H_{97}O_{21}$, 1189.6522), 1211.6338 $[M+Na]^+$ (calcd for $C_{63}H_{96}O_{21}Na$, 1211.6342).

2.3.3. Calotroposide J (**3**)

Brown viscous residue; $[\alpha]_D$ + 7.4 (*c* 1.1, MeOH); UV (MeOH) λ_{max} (log ε): 230 (4.06), 272 (3.14), 280 (3.05) nm; IR (KBr) ν_{max}: 3480, 2933, 1710, 1640, 1455, 1100, 1055 cm^{-1}; NMR data, see Tables 1–4; HRESIMS *m/z*: 1391.7005 $[M-H]^+$ (calcd for $C_{71}H_{107}O_{27}$, 1391.7000).

2.3.4. Calotroposide K (**4**)

Brown viscous residue; $[\alpha]_D$ + 8.1 (*c* 1.1, MeOH); UV (MeOH) λ_{max} (log ε): 230 (4.05), 273 (3.16), 280 (3.05) nm; IR (KBr) ν_{max}: 3510, 2930, 1710, 1630, 1450, 1275, 1100, 1055 cm^{-1}; NMR data, see Tables 1–4; HRESIMS *m/z*: 1349.6892 $[M-H]^+$ (calcd for $C_{69}H_{105}O_{26}$, 1349.6894).

2.3.5. Calotroposide L (**5**)

Brown viscous residue; $[\alpha]_D$ + 12.7 (*c* 1.1, MeOH); UV (MeOH) λ_{max} (log ε): 230 (4.09), 270 (3.10), 280 (3.11) nm; IR (KBr) ν_{max}: 3485, 2933, 1710, 1600, 1450, 1270, 1100, 1055 cm^{-1}; NMR data, see Tables 1–4; HRESIMS *m/z*: 1367.6632 $[M-H]^+$ (calcd for $C_{68}H_{103}O_{28}$, 1367.6636).

2.3.6. Calotroposide M (**6**)

Brown viscous residue; $[\alpha]_D$ + 17.1 (*c* 1.1, MeOH); UV (MeOH) λ_{max} (log ε): 230 (4.12), 273 (3.16), 280 (3.09) nm; IR (KBr) ν_{max}: 3560, 2942, 1720, 1645, 1455, 1100, 1055 cm^{-1}; NMR data, see Tables 1–4; HRESIMS *m/z*: 1537.7941 $[M+H]^+$ (calcd for $C_{78}H_{121}O_{30}$, 1537.7943).

2.3.7. Calotroposide N (**7**)

Brown viscous residue; $[\alpha]_D$ + 22.9 (*c* 1.1, MeOH); UV (MeOH) λ_{max} (log ε): 230 (4.07), 270 (3.10), 280 (3.12) nm; IR (KBr) ν_{max}: 3530, 2925, 1710, 1610, 1450, 1275, 1110, 1055 cm^{-1}; NMR data, see Tables 1–4; HRESIMS *m/z*: 1511.7418 $[M-H]^+$ (calcd for $C_{75}H_{115}O_{31}$, 1511.7422).

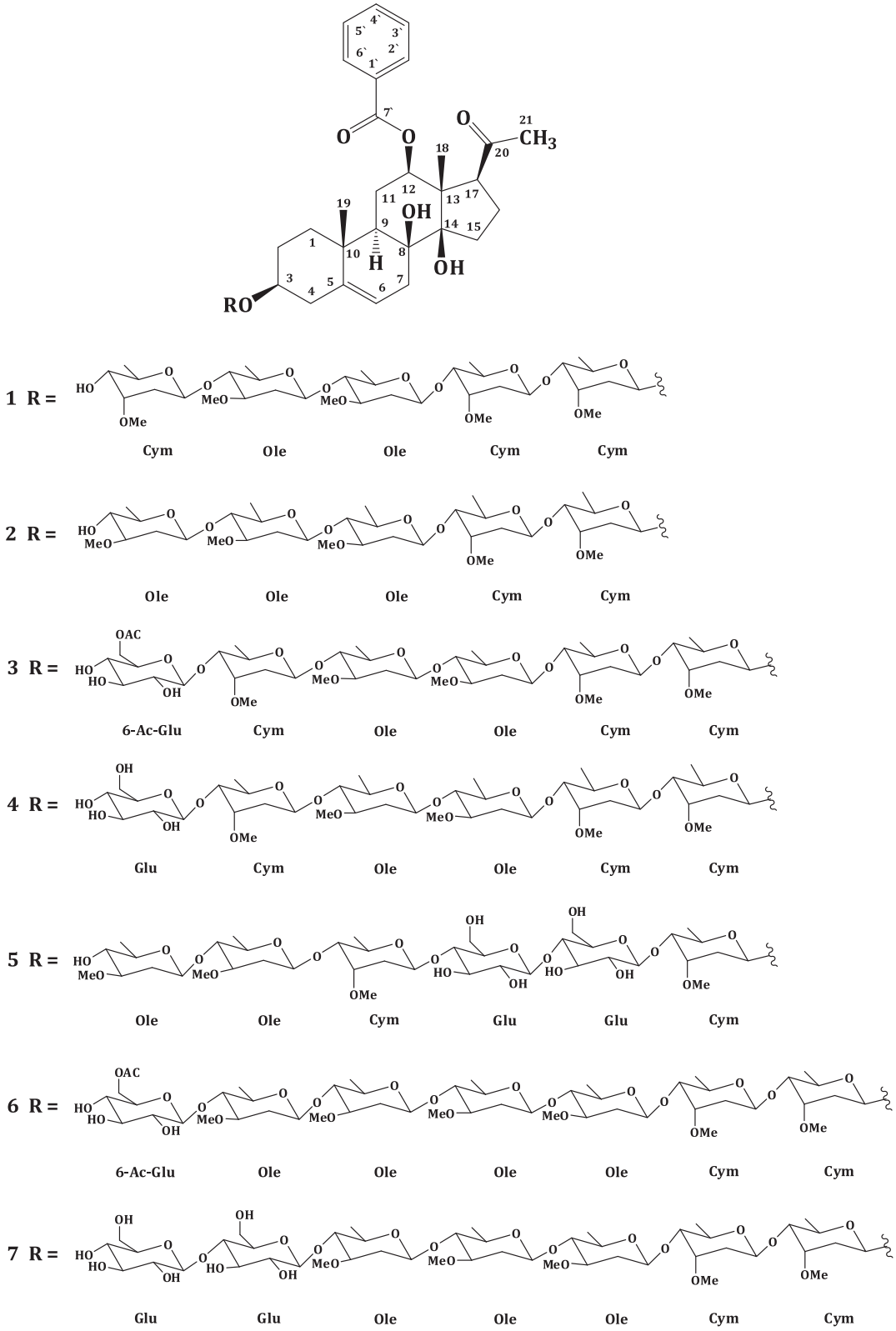

Fig. 1. Structures of the isolated compounds **1–7**.

2.4. Acid hydrolysis and determination of the absolute configuration of the sugar moieties

A solution of the isolated glycosides (**1–7**) (8 mg in 6 mL MeOH each) was treated with 0.2 N H_2SO_4 (1.5 mL) and heated at 60 °C for 4 h. After hydrolysis, the reaction mixture was diluted with H_2O and extracted with $CHCl_3$. The aqueous layer was de-acidified, concentrated, and passed through Sephadex LH-20 eluted with MeOH to remove the salts, then silica gel column using $CHCl_3$:-MeOH:H_2O (7:1:1.2) system to obtain oleandrose, cymarose, and

Table 1
^{1}H NMR data (400 MHZ) for aglycone moieties of compounds **1–7** (δ in ppm, DMSO-d_6, J in Hz).

H	1	2	3	4	5	6	7
1	1.71 m	1.71 m	1.71 m	1.72 m	1.73 m	1.72 m	1.72 m
	1.10 m	1.08 m	1.09 m	1.21 m	1.08 m	1.21 m	1.10 m
2	1.75 m	1.75 m	1.76 m	1.74 m	1.72 m	1.75 m	1.75 m
	1.28 m	1.40 m	1.43 m	1.32 m	1.22 m	1.25 m	1.21 m
3	3.71 m	3.74 m	3.79 m	3.71 m	3.62 m	3.69 m	3.71 m
4	2.32 m	2.33 m	2.31 m	2.31 m	2.31 m	2.36 m	2.27 m
	2.12 m	2.11 m	2.13 m	2.05 m	1.71 m	1.72 m	2.03 m
6	5.28 brs	5.28 brs	5.29 brs	5.29 brs	5.29 brs	5.29 brs	5.29 brs
7	2.03 m	2.05 m	2.05 m	2.05 m	2.05 m	2.00 m	2.03 m
9	1.49 dd (12.8, 2.8)	1.48 dd (12.9, 2.8)	1.48 dd (12.8, 3.3)	1.49 dd (12.9, 2.8)	1.49 dd (12.2, 3.2)	1.48 dd (12.7, 3.3)	1.46 dd (12.5, 2.9)
11	1.86 m	1.83 m	1.86 m	1.87 m	1.83 m	1.88 m	1.85 m
	1.68 m	1.68 m	1.69 m	1.65 m	1.64 m	1.67 m	1.62 m
12	4.87 dd (12.0, 4.0)	4.76 dd (12.0, 3.8)	4.93 dd (11.8, 4.1)	4.78 dd (11.8, 4.1)	4.77 dd (11.2, 4.0)	4.74 dd (12.0, 4.1)	4.75 dd (11.9, 4.2)
15	1.89 m	1.93 m	1.95 m	1.98 m	1.89 m	1.99 m	1.86 m
	1.59 m	1.57 m	1.59 m	1.61 m	1.62 m	1.58 m	1.64 m
16	2.03 m	2.01 m	2.01 m	2.08 m	2.04 m	1.98 m	2.10 m
	1.63 m	1.64 m	1.63 m	1.65 m	1.70 m	1.58 m	1.68 m
17	3.20 dd (9.5, 5.5)	3.19 dd (9.5, 5.3)	3.19 dd (9.6, 5.4)	3.18 dd (9.5, 5.6)	3.20 dd (9.5, 5.3)	3.15 dd (9.6, 5.1)	3.20 dd (9.5, 5.5)
18	1.59 s	1.59 s	1.59 s	1.60 s	1.59 s	1.59 s	1.59 s
19	1.03 s	1.03 s	1.05 s	1.07 s	1.06 s	1.05 s	1.06 s
21	1.98 s	1.98 s	1.96 s	1.97 s	1.96 s	1.96 s	1.96 s
2′, 6′	7.88 dd (8.0, 1.6)	7.86 dd (8.0, 1.6)	7.86 dd (8.0, 1.6)	7.87 dd (8.0, 1.6)	7.87 dd (8.0, 1.6)	7.86 dd (8.0, 1.6)	7.87 dd (8.0, 1.6)
3′, 5′	7.52 t (8.0)	7.51 t (8.0)	7.51 t (8.0)	7.51 t (8.0)	7.51 t (8.0)	7.51 t (8.0)	7.51 t (8.0)
4′	7.65 dt (8.0, 1.6)	7.63 t (8.0)	7.64 dt (8.0, 1.6)	7.63 t (8.0)	7.63 t (8.0)	7.64 dt (8.0, 1.6)	7.63 t (8.0)

Table 2
^{13}C NMR Data (100 MHz) of aglycone moieties of compounds **1–7** (δ in ppm, DMSO-d_6).[a]

C	1	2	3	4	5	6	7
1	38.6, CH_2	38.3, CH_2	38.0, CH_2	38.2, CH_2	37.5, CH_2	38.1, CH_2	38.2, CH_2
2	29.3, CH_2	28.8, CH_2	28.8, CH_2	30.5, CH_2	29.0, CH_2	28.8, CH_2	29.1, CH_2
3	77.0, CH	76.5, CH	76.3, CH	76.7, CH	76.9, CH	76.3, CH	76.4, CH
4	38.8, CH_2	38.0, CH_2	38.1, CH_2	38.3, CH_2	38.1, CH_2	37.9, CH_2	38.0, CH_2
5	138.7, C	138.1, C	137.9, C	138.2, C	138.4, C	137.9, C	138.0, C
6	119.2, CH	118.9, CH	118.8, CH	119.0, CH	119.4, CH	118.8, CH	118.7, CH
7	33.8, CH_2	34.1, CH_2	34.1, CH_2	34.3, CH_2	34.6, CH_2	34.1, CH_2	33.7, CH_2
8	73.9, C	75.1, C	73.3, C	73.6, C	73.6, C	73.5, C	73.6, C
9	43.9, CH	43.3, CH	43.2, CH	43.5, CH	43.5, CH	43.2, CH	43.3, CH
10	37.3, C	36.4, C	36.4 s	35.6, C	35.5, C	35.5, C	35.3, C
11	24.3, CH_2	23.8, CH_2	23.8, CH_2	24.0, CH_2	24.2, CH_2	23.7, CH_2	23.8, CH_2
12	73.2, CH	73.4, CH	72.6, CH	72.8, CH	73.4, CH	73.4, CH	73.4, CH
13	55.3, C	54.9, C	54.8, C	55.0, C	55.1, C	54.8, C	54.8, C
14	87.0, C	86.6, C	86.4, C	86.7, C	86.8, C	86.5, C	86.5, C
15	34.0, CH_2	33.3, CH_2	33.1, CH_2	33.4, CH_2	33.4, CH_2	33.1, CH_2	33.4, CH_2
16	21.5, CH_2	23.8, CH_2	23.8, CH_2	24.0, CH_2	23.6, CH_2	23.7, CH_2	23.8, CH_2
17	58.0, CH	58.5, CH	59.8, CH	58.0, CH	59.3, CH	57.8, CH	57.9, CH
18	15.6, CH_3	15.2, CH_3	15.1, CH_3	15.2, CH_3	15.2, CH_3	15.3, CH_3	15.1, CH_3
19	18.0, CH_3	17.6, CH_3	17.5, CH_3	17.7, CH_3	17.8, CH_3	17.5, CH_3	17.6, CH_3
20	209.6, C	209.5, C	209.6, C	209.7, C	209.7, C	209.3, C	209.3, C
21	32.3, CH_3	32.5, CH_3	31.9, CH_3	32.1, CH_3	32.4, CH_3	31.9, CH_3	31.9, CH_3
1′	130.5, C	129.9, C	129.8, C	130.0, C	130.0, C	129.8, C	129.8, C
2′, 6′	129.5, CH	129.1, CH	128.9, CH	129.2, CH	129.2, CH	128.9, CH	129.0, CH
3′, 5′	129.0, CH	128.6, CH	128.5, CH	128.8, CH	128.8, CH	128.6, CH	128.6, CH
4′	133.5, CH	133.2, CH	133.1, CH	133.3, CH	132.7, CH	133.1, CH	133.2, CH
7′	164.7, C	164.3, C	164.1, C	164.5, C	164.5, C	164.2, C	164.2, C

[a] Carbon multiplicities were determined by HSQC experiments, C = quaternary carbon, CH = methine, CH_2 = methylene, CH_3 = methyl carbons.

glucose. Each sugar was dissolved in pyridine (0.3 mL) and treated with 0.5 mL bis(trimethylsilyl)trifluoroacetamide for 15 min at room temperature. Silylated sugars were subjected to GCMS analysis on Clarus 500 GC/MS to determine the sugars (see Section 2). They were identified as D-oleandrose (t_R = 12.6 min), cymarose (t_R = 12.1 min), and D-glucose (t_R = 12.3 min) by comparison with authentic samples. The absolute configuration of all the monosaccharide sugars was D-form based on their optical rotation and comparison with literature as follows; D-cymarose: $[\alpha]_D$ + 52.4 (*c* 0.15, H_2O, 24 h) (Lit. $[\alpha]_D$ + 52.6 (*c* 0.15, H_2O, 24 h); D-oleandrose: $[\alpha]_D$ − 12.7 (*c* 0.18, H_2O, 24 h) (Lit. $[\alpha]_D$ − 12.8 (*c* 0.18, H_2O, 24 h); D-glucose: $[\alpha]_D$ + 51.0 (*c* 0.2, H_2O, 24 h) (Lit. $[\alpha]_D$ + 50.0 (*c* 0.2, H_2O, 24 h) [13,14].

The $CHCl_3$ layer was concentrated and subjected to SiO_2 column chromatography (30 g × 20 cm × 1 cm) using *n*-hexane:EtOAc gradient to give 12-*O*-benzoylisolineolon. ^{1}H NMR ($CDCl_3$, 600 MHz): δ_H 1.19 (3H, s, H_3-19), 1.27 (3H, s, H_3-18), 3.11 (1H, dd, J = 9.5, 5.5 Hz, H-17), 4.50 (1H, m, H-3), 4.62 (1H, dd, J = 12.1, 4.0 Hz, H-12), 5.38 (1H, brd, J = 3.0 Hz, H-6), 7.55 (2H, brd, J = 8.0 Hz, H-2′, 6′), 7.48 (1H, t, J = 8.0 Hz, H-4′), 7.43 (2H, brt, J = 8.0 Hz, H-3′, 5′).

2.5. Determination of in vitro cancer growth inhibitory activity

The *in vitro* cancer growth inhibitory activity of the *n*-BuOH fraction and isolated compounds was determined using MTT colorimetric assay against the A549 NSCLC (Deutsche Sammlung von

Table 3
^{1}H NMR data (400 MHz) for sugar moieties of compounds **1–7** (δ in ppm, DMSO-d_6, J in Hz).

H	1	2	3	4	5	6	7
Sug-1	Cym.	Cym.	Cym.	Cym.	Cym.	Cym.	Cym.
1	4.75 dd (9.5, 2.5)	4.74 dd (9.5, 2.4)	4.75 dd (9.5, 2.5)	4.75 dd (9.5, 2.4)	4.75 dd (9.5, 2.2)	4.75 dd (9.5, 2.5)	4.77 dd (9.5, 2.4)
2	1.90 m	1.90 m	1.91 m	1.90 m	1.91 m	1.92 m	1.90 m
	1.44 m	1.44 m	1.45 m	1.47 m	1.44 m	1.44 m	1.45 m
3	3.68 m	3.68 m	3.65 m	3.66 m	3.67 m	3.66 m	3.68 m
4	3.11 m	3.08 m	3.07 m	3.20 m	3.20 m	3.08 m	3.09 m
5	3.66 m	3.66 m	3.66 m	3.68 m	3.74 m	3.72 m	3.72 m
6	1.06 d (6.3)	1.08 d (6.3)	1.08 d (6.0)	1.09 d (6.1)	1.18 d (6.0)	1.12 d (6.2)	1.10 d (6.2)
3-OCH_3	3.33 s	3.33 s	3.32 s	3.34 s	3.34 s	3.30 s	3.34 s
Sug-2	Cym.	Cym.	Cym.	Cym.	Glu.	Cym.	Cym.
1	4.69 dd (9.6, 2.5)	4.69 dd (9.3, 2.5)	4.69 dd (9.5, 2.2)	4.61 dd (9.5, 2.4)	4.40 d (7.6)	4.62 dd (9.5, 2.5)	4. 83 dd (9.5, 2.4)
2	1.94 m	1.95 m	1.93 m	1.92 m	2.99 m	1.94 m	1.92 m
	1.42 m	1.45 m	1.43 m	1.48 m		1.45 m	1.44 m
3	3.65 m	3.65 m	3.65 m	3.67 m	3.07 m	3.68 m	3.68 m
4	3.12 m	3.11 m	3.10 m	3.18 m	3.23 m	3.10 m	3.10 m
5	3.70 m	3.72 m	3.67 m	3.71 m	3.31 m	3.68 m	3.70 m
6	1.12 d (6.3)	1.11 d (6.5)	1.10 d (6.3)	1.12 d (6.0)	3.63 m	1.09 d (6.5)	1.08 d (6.4)
					3.43 m		
3-OCH_3	3.32 s	3.32 s	3.31 s	3.33 s	–	3.30 s	3.34 s
Sug-3	Ole.	Ole.	Ole.	Ole.	Glu.	Ole.	Ole.
1	4.61 dd (10.0, 2.0)	4.61 dd (10.5, 2.0)	4.58 dd (10.1, 2.0)	4.68 dd (10.2, 2.0)	4.28 d (7.2)	4.71 dd (10.0, 2.0)	4.52 dd (10.1, 2.0)
2	2.04 m	2.08 m	2.20 m	2.07 m	3.01 m	2.08 m	2.06 m
	1.42 m	1.73 m	1.73 m	1.72 m		1.74 m	1.72 m
3	3.15 m	3.15 m	3.18 m	3.15 m	3.03 m	3.16 m	3.17 m
4	3.23 m	3.21 m	3.25 m	3.25 m	3.25 m	3.19 m	3.24 m
5	3.19 m	3.26 m	3.16 m	3.28 m	3.34 m	3.22 m	3.26 m
6	1.19 d (6.5)	1.20 d (6.3)	1.21 d (6.2)	1.27 d (6.0)	3.67 m	1. 22 d (6.2)	1.19 (6.1)
					3.45 m		
3-OCH_3	3.29 s	3.29 s	3.29 s	3.32 s	-	3.33 s	3.29 s
Sug-4	Ole.	Ole.	Ole.	Ole.	Cym.	Ole.	Ole.
1	4.55 dd (10.1, 2.0)	4.58 dd (10.4, 2.1)	4.61 dd (10.2, 2.1)	4.53 dd (10.0, 2.0)	4.69 dd (9.5, 2.4)	4.56 dd (10.2, 2.0)	4.70 dd (10.1, 2.0)
2	2.08 m	2.10 m	2.03 m	2.10 m	2.00 m	2.05 m	2.09 m
	1.75 m	1.73 m	1.73 m	1.73 m	1.74 m	1.72 m	1.74 m
3	3.20 m	3.15 m	3.21 m	3.11 m	3.69 m	3.20 m	3.15 m
4	3.25 m	3.23 m	3.23 m	3.22 m	3.20 m	3.28 m	3.30 m
5	3.18 m	3.18 m	3.12 m	3.21 m	3.70 m	3.18 m	3.20 m
6	1.17 d (6.3)	1.22 d (6.3)	1.18 d (6.5)	1.20 d (6.4)	1.10 d (6.6)	1.28 d (6.4)	1.28 d (6.4)
3-OCH_3	3.31 s	3.30 s	3.30 s	3.35 s	3.34 s	3.33 s	3.29 s
Sug-5	Cym.	Ole.	Cym.	Cym.	Ole.	Ole.	Ole.
1	4.77 dd (9.5, 2.4)	4.47 dd (10.2, 2.1)	4.87 dd (9.5, 2.2)	4.78 dd (9.5, 2.5)	4.61 dd (10.2, 2.0)	4.52 dd (10.2, 2.2)	4.63 dd (10.1, 1.0)
2	1.95 m	2.15 m	1.94 m	1.97 m	2.29 m	2.15 m	2.22 m
	1.51 m	1.75 m	1.50 m	1.49 m	1.75 m	1.70 m	1.78 m
3	3.71 m	3.15 m	3.69 m	3.25 m	3.09 m	3.15 m	3.18 m
4	3.35 m	3.18 m	3.12 m	3.22 m	3.18 m	3.21 m	3.22 m
5	3.31 m	3.28 m	3.70 m	3.68 m	3.22 m	3.22 m	3.28 m
6	1.06 d (6.3)	1.18 d (6.3)	1.12 d (6.2)	1.11 d (6.1)	1.15 d (6.3)	1.13 d (6.3)	1.23 d (6.4)
3-OCH_3	3.33 s	3.32 s	3.33 s	3.31 s	3.31 s	3.33 s	3.29 s
Sug-6	–	–	6-*O*-Ac-Glu.	Glu.	Ole.	Ole.	Glu.
1	–	–	4.18 d (7.2)	4.21 d (7.6)	4.56 dd (10.2, 2.0)	4.38 dd (10.1, 2.5)	4.27 d (7.8)
2	–	–	2.95 m	2.95 m	2.21 m	2.12 m	2.98 m
					1.73 m	1.75 m	
3	–	–	3.09 m	3.12 m	3.15 m	3.22 m	3.15 m
4	–	–	3.00 m	3.05 m	3.09 m	3.20 m	3.32 m
5	–	–	3.16 m	3.35 m	3.25 m	3.26 m	3.20 m
6	–	–	4.49 m	3.64 m	1.15 d	1.19 d	3.71 m
			4.17 m	3.41 m	(6.3)	(6.8)	3.44 m
3-OCH_3	–	–	–	–	3.31 s	3.33 s	
6-OAc	–	–	1.98 s				
Sug-7	–	–	–	–	–	6-*O*-Ac-Glu.	Glu.
1	–	–	–	–	–	4.26 d (7.8)	4.40 d (7.8)
2	–	–	–	–	–	2.99 m	2.97 m
3	–	–	–	–	–	3.17 m	3.08 m
4	–	–	–	–	–	3.03 m	3.06 m
5	–	–	–	–	–	3.15 m	3.18 m
6	–	–	–	–	–	4.48 m	3.72 m
						4.16 m	3.42 m
6-OAc	–	–	–	–	–	1.91 s	–

Mikroorganismen and Zellkulturen, DSMZ; code ACC107), PC-3 prostate cancer (DSMZ; code ACC465), and U373 GBM (European Collection of Cell Culture, ECACC; code 89081403) cancer cell lines as previously outlined [6,11,12].

Table 4
^{13}C NMR Data (100 MHz) for Sugar Moieties of Compounds **1–7** (δ in ppm, DMSO-d_6).[a]

C	1	2	3	4	5	6	7
Sug-1	Cym.	Cym.	Cym.	Cym.	Cym.	Cym.	Cym.
1	95.7, CH	95.2, CH	95.0, CH	95.3, CH	95.3, CH	95.1, CH	95.7, CH
2	36.2, CH_2	35.8, CH_2	35.7, CH_2	36.6, CH_2	35.6, CH_2	36.4, CH_2	35.6, CH_2
3	76.8, CH	76.2, CH	76.5, CH	76.7, CH	76.5, CH	76.6, CH	76.5, CH
4	82.2, CH	81.8, CH	81.9, CH	81.7, CH	82.1, CH	82.4, CH	82.4, CH
5	68.4, CH	68.0, CH	67.6, CH	68.1, CH	68.1, CH	68.4, CH	67.8, CH
6	18.9, CH_3	17.6, CH_3	17.6, CH_3	17.7, CH_3	17.9, CH_3	18.1, CH_3	18.2, CH_3
3-OCH_3	59.6, CH_3	57.9, CH_3	57.6, CH_3	58.0, CH_3	59.3, CH_3	60.5, CH_3	59.1, CH_3
Sug-2	Cym.	Cym.	Cym.	Cym.	Glu.	Cym.	Cym.
1	99.6, CH	96.9, CH	99.3, CH	99.5, CH	103.0, CH	98.9, CH	97.8, CH
2	36.8, CH_2	35.5, CH_2	36.4, CH_2	36.6, CH_2	75.2, CH	36.4, CH_2	36.1, CH_2
3	77.1, CH	76.8, CH	76.6, CH	77.1, CH	75.0, CH	76.7, CH	77.0, CH
4	82.6, CH	82.0, CH	82.9, CH	82.2, CH	80.7, CH	82.3, CH	81.9, CH
5	68.5, CH	69.7, CH	67.9, CH	68.0, CH	76.9, CH	69.9, CH	69.1, CH
6	18.7, CH_3	17.6, CH_3	17.9, CH_3	17.8, CH_3	61.4, CH_2	18.1, CH_3	18.0, CH
3-OCH_3	58.4, CH_3	57.9, CH_3	57.8, CH_3	57.7, CH_3	-	59.0, CH_3	57.8, CH_3
Sug-3	Ole.	Ole.	Ole.	Ole.	Glu.	Ole.	Ole.
1	99.8, CH	99.4, CH	99.3, CH	99.2, CH	103.6, CH	99.3, CH	98.9, CH
2	36.8, CH_2	36.5, CH_2	36.4, CH_2	36.6, CH_2	76.8, CH	37.4, CH_2	35.8, CH_2
3	76.8, CH	76.7, CH	76.6, CH	76.8, CH	74.9, CH	76.7, CH	76.8, CH
4	82.4, CH	82.1, CH	82.2, CH	82.0, CH	80.6, CH	81.9, CH	80.5, CH
5	70.3, CH	71.7, CH	70.1, CH	70.6, CH	77.2, CH	72.6, CH	69.3, CH
6	18.6, CH_3	17.6, CH_3	18.0, CH_3	18.1, CH_3	60.8, CH_2	18.0, CH_3	18.0, CH_3
3-OCH_3	56.5, CH_3	56.5, CH_3	56.4, CH_3	56.6, CH_3	-	57.6, CH_3	56.4, CH_3
Sug-4	Ole.	Ole.	Ole.	Ole.	Cym.	Ole.	Ole.
1	101.1, CH	100.1, CH	100.6, CH	100.9, CH	99.7, CH	100.6, CH	100.8, CH
2	36.9, CH_2	36.4, CH_2	36.4, CH_2	35.8, CH_2	35.7, CH_2	35.6, CH_2	36.5, CH_2
3	77.3, CH	77.3, CH	76.7, CH	76.7, CH	76.7, CH	76.5, CH	77.3, CH
4	82.3, CH	81.8, CH	82.2, CH	82.2, CH	82.2, CH	82.0, CH	80.5, CH
5	70.8, CH	70.3, CH	70.1, CH	69.8, CH	68.2, CH	70.6, CH	69.9, CH
6	18.5, CH_3	18.2, CH_3	18.1, CH_3	17.9, CH_3	18.2, CH_3	18.0, CH_3	18.0, CH_3
3-OCH_3	56.4, CH_3	56.5, CH_3	56.4, CH_3	59.3, CH_3	59.3, CH_3	56.4, CH_3	56.3, CH_3
Sug-5	Cym.	Ole.	Cym.	Cym.	Ole.	Ole.	Ole.
1	97.9, CH	100.8, CH	96.9, CH	97.6, CH	99.6, CH	100.6, CH	99.3, CH
2	37.2, CH_2	36.9, CH_2	36.4, CH_2	35.6, CH_2	35.6, CH_2	36.4, CH_2	36.5, CH_2
3	76.7, CH	79.9, CH	76.5, CH	76.8, CH	76.9, CH	76.5, CH	77.3, CH
4	73.9, CH	73.9, CH	81.9, CH	82.2, CH	82.3, CH	81.9, CH	80.9, CH
5	70.9, CH	70.4, CH	68.4, CH	68.2, CH	70.2, CH	72.6, CH	70.2, CH
6	19.0, CH_3	17.6, CH_3	17.8, CH_3	18.1, CH_3	18.2, CH_3	18.0, CH_3	18.0, CH_3
3-OCH_3	58.4, CH_3	57.0, CH_3	59.0, CH_3	56.8, CH_3	56.5, CH_3	56.2, CH_3	56.4, CH_3
Sug-6	–	–	6-O-Ac-Glu.	Glu.	Ole.	Ole.	Glu.
1	–	–	104.8, CH	104.9, CH	100.9, CH	102.6, CH	103.1, CH
2	–	–	74.7, CH	73.8, CH	35.8, CH_2	36.4, CH_2	73.7, CH
3	–	–	77.8, CH	76.8, CH	82.3, CH	74.6, CH	76.4, CH
4	–	–	73.3, CH	72.8, CH	76.6, CH	81.9, CH	81.9, CH
5	–	–	77.8, CH	78.1, CH	70.2, CH	71.0, CH	76.4, CH
6	–	–	64.3, CH_2	61.5, CH_2	18.2, CH_3	18.0, CH_3	61.0, CH_2
3-OCH_3	–	–	–	–	56.7, CH_3	57.7, CH_3	–
6-OAc	–	–	173.0, C 20.7, CH_3	–	–	–	–
Sug-7	–	–	–	–	–	6-O-Ac-Glu.	Glu.
1	–	–	–	–	–	103.1, CH	102.6, CH
2	–	–	–	–	–	74.6, CH	73.3, CH
3	–	–	–	–	–	76.8, CH	77.8, CH
4	–	–	–	–	–	72.6, CH	70.0, CH
5	–	–	–	–	–	78.1, CH	77.8, CH
6	–	–	–	–	–	63.9, CH_2	60.6, CH_2
6-OAc	–	–	–	–	–	173.0, C 21.0, CH_3	–

[a] Carbon multiplicities were determined by HSQC experiments, C = quaternary carbon, CH = methine, CH_2 = methylene, CH_3 = methyl carbons.

3. Results and discussion

The air-dried powdered root bark was extracted with MeOH. The MeOH extract was partitioned between *n*-hexane, $CHCl_3$, EtOAc, and *n*-BuOH. The *n*-BuOH fraction was subsequently separated on normal SiO_2 column, Sephadex LH-20, RP-18, and semi-preparative HPLC to provide seven compounds **1–7**.

Compounds **1–7** gave positive Libermann-Burchard and Keller-Kiliani reactions indicating their steroidal skeleton with a 2-deoxy sugar moiety [15]. Compounds **1–7** showed the presence of benzoyl moiety at C-12 and a straight sugar chain consists of 5–7 units connected to C-3 of the aglycone. The benzoylation of the OH at C-12 was confirmed from the downfield shifts of their corresponding protons and carbons, as well as the HMBC experiment which showed correlation from H-12 of the aglycone moiety to the carbonyl carbon of the benzoyl group. The IR spectra showed characteristic bands for OH and C=O groups, whereas the UV spectra showed absorption maxima at 230, 272, and 280 nm suggesting

the presence of a benzoyl moiety [16]. The relative stereochemistry at the chiral centers of the aglycone moiety was deduced from comparison of carbons chemical shifts and protons coupling constants with those of previously reported and related oxypregnanes.

The aglycone of compounds **1–7** could be 12-*O*-benzoyllineolon or 12-*O*-benzoylisolineolon, which are epimer differing in the orientation at position-17. The relative configuration at C-17 can be attributed on the basis of the ^{1}H and ^{13}C NMR chemical shifts and *J* value of H-17. The α-configured H-17 resonates at 3.22–3.27 ppm (dd, *J* = 9.2–9.5 and 5.5–5.8 Hz) together with C-17 chemical shift at 56.2–59.5 ppm [13,17–20], while the β-configured H-17 resonates at δ_H 3.42–3.55 (*J* = 9.5 Hz) with 60.1–60.7 ppm for C-17 [16,21–23].

In addition, the benzoylisolineolon-related oxypregnane glycosides with α-configured H-17 possess a positive optical rotation values, while those with derivatives negative optical rotation values possess *β*-configured H-17. Accordingly, the aglycone of **1–7** was considered to be 12-*O*-benzoylisolineolon. A detailed 1D and 2D NMR spectroscopic analyses of **1–7** (Tables 1–4) and comparison to the data of the previously isolated oxypregnane glycosides allowed the identification of the aglycone moiety of **1–7** as 12-*O*-benzoylisolineolon [13,17–19]. This was confirmed by acid hydrolysis of the glycosides followed by ^{1}H NMR and $[\alpha]_D$ measurements of the corresponding aglycones. The identification of the monosaccharides in the hydrolysates of compounds **1–7** was confirmed by co-TLC with authentic sugars as well as comparison of the GCMS retention times with standards monosaccharides. The absolute configuration of the deoxy sugars was determined to be D-forms by comparison of ^{13}C NMR data and optical rotation with those of the corresponding sugars [16,21–24]. A survey of closely related glycosides revealed that all the *β*-linked 2,6-dideoxy sugars have the D-configuration, whereas the α-linked sugars are mostly L-configured. An analysis of the ^{13}C chemical shift values for C-2 of 2-deoxy sugars (cymaropyranose and oleandropyranose) of a large number of steroid glycosides revealed that C-2 of *β*-D-sugars resonates at 35.0–38.0 ppm and that of α-D-sugars appears at 35.0–36.0 ppm whereas the corresponding carbon atom (C-2) of α-L-sugar appears at 30.0–32.0 ppm [14]. The chemical shift values for C-2 of cymaropyranose and oleandropyranose moieties (Table 4) confirmed their D-configuration together with their optical rotation values and by comparing their data with related compounds in the literatures [22–24]. All sugar linkages in the glycosides were assigned to be *β*-form based on the large coupling constant values of their anomeric protons as shown in table 3. The observed *J* values for cymaropyranose were 9.3–9.6 and 2.2-2.5 Hz, 10.0–10.5 and 2.0–2.5 Hz for oleandropyranose, and 7.2–7.8 Hz for glucopyranose indicating the *β*-configuration of the previously mentioned sugars [22–24]. It was also reported that the C-1 of the inner cymaropyranose unit is characteristically resonating up-field around 95.0–95.9 ppm when linked to C-3 of the aglycone in contrast to C-1 of a terminal cymaropyranose (97.8–100.4 ppm) when linked to a sugar unit [14]. To the best of our knowledge, compounds **1–7** were isolated here for the first time from nature and their structures were determined by careful inspection of 1D, 2D NMR, and HRESIMS spectroscopic data, in addition to, acid hydrolysis followed by GCMS and optical rotations measurement of the purified monosaccharides and ^{1}H NMR spectral analysis of aglycone.

Compound **1** was isolated as brown viscous residue. It had a molecular formula $C_{63}H_{96}O_{21}$ on the basis of HRESIMS quasi-molecular ion peaks at *m/z* 1189.6519 $[M+H]^+$ and 1211.6348 $[M+Na]^+$ confirmed by ^{13}C NMR and multiplicity-edited HSQC spectral data. Also, the ESIMS spectrum of **1** revealed the presence of prominent fragment ion peaks at *m/z* 1084.3 [(M+H)-105 (benzoyl group)]$^+$, 939.6 [(M+H)-250 (benzoyl group + Cym)]$^+$, and 795.2 [(M+H)-394 (benzoyl group + Cym + Ole)]$^+$. The IR spectrum showed absorption bands at 3435 and 1714 cm^{-1} for hydroxyl and ketone functionalities, respectively. The UV spectrum showed absorption maxima at 215, 225, and 278 nm, which are consistent with the presence of aromatic ring in **1**. The NMR spectra exhibited signals characteristic of an oxypregnane oligoglycoside containing cymarose and oleandrose moieties [13,18,19,25]. The ^{1}H and ^{13}C NMR spectra of **1** displayed signals for three methyls at δ_H 1.98 (s, H_3-21)/δ_C 32.3 (C-21), 1.59 (s, H_3-18)/δ_C 15.6 (C-18), and 1.03 (s, H_3-19)/δ_C 18.0 (C-19), and *tri*-substituted olefinic double bond at δ_H 5.28 (s, H-6)/δ_C 119.2 (C-6) and 138.7 (C-5) characteristic of the pregn-5-en-20-one skeleton [13,18,19,25]. The $^{3}J_{CH}$ HMBC correlations of H-6 with C-8 (δ_C 73.9) and C-10 (δ_C 37.3) and H-3 and H_3-19 with C-5 (δ_C 138.7) confirmed the position of the double bond between C-5 and C-6. The NMR signals at δ_H 7.88 (dd, *J* = 8.0, 1.6 Hz, H-2′, 6′)/δ_C 129.5, 7.52 (t, *J* = 8.0 Hz, H-3′, 5′)/δ_C 129.0, 7.65 (dt, *J* = 8.0, 1.6 Hz, H-4′)/δ_C 133.5, 130.5 (C-1′), and 164.7 (C-7′) are characteristic for a benzoyl moiety. This moiety was established by ^{1}H–^{1}H COSY correlation and further secured by the HMBC cross peaks of H-2′ and H-6′ with C-1′, C-4′, and C-7′, H-4′ to C-2′ and C-6′, and H-3′ and H-5′ to C-1′ and C-4′. The location of the benzoyl moiety at C-12 was secured by the HMBC correlation between H-12 and C-7′ (δ_C 164.7). Moreover, resonances for two oxymethine groups of the aglycone moiety were observed at δ_H 3.71 (1H, m, H-3)/δ_C 77.0 (C-3) and δ_H 4.87 (1H, dd, *J* = 12.0, 4.0 Hz, H-12)/δ_C 73.2 (C-12). Their positions at C-3 and C-12 were established based on the HMBC correlations of H-1 and H-4 to C-3 (δ_C 77.0) and H-9 and H_3-18 to C-12 (δ_C 73.2). Furthermore, the ^{13}C NMR exhibited two oxygenated quaternary carbons at δ_C 73.9 (C-8) and 87.0 (C-14). The assignment of these carbon was supported by HMBC cross peaks of H-6/C-8, H-15/C-8, H-17/C-14, and H_3-18/C-14. The presence of an acetyl group was evident from the signals resonating at δ_H 1.98 (H-21)/δ_C 32.3 (C-21) and 209.6 (C-20). Its connectivity to C-17 was established based on HMBC cross peaks from H-17 to C-20 and H_3-21 to C-17. The signals at δ_H 3.20 (dd, *J* = 9.5, 5.5 Hz)/δ_C 58.0 were assigned to H-17α, which was confirmed by the HMBC cross peaks of H-12, H-15, and H-18 to C-17. The comparison of the NMR data (Tables 1 and 2) of **1** with those reported for similar compounds supported the assignment of aglycone as 12-*O*-benzoylisolineolon [13,17–20]. Five anomeric signals were observed in the ^{1}H and ^{13}C NMR spectra at δ_H/δ_C 4.75 (dd, *J* = 9.5, 2.5 Hz)/95.7, 4.69 (dd, *J* = 9.6, 2.5 Hz)/99.6, 4.61 (dd, *J* = 10.0, 2.0 Hz)/99.8, 4.55 (dd, *J* = 10.1, 2.0 Hz)/101.1, and 4.77 (dd, *J* = 9.5, 2.4 Hz)/97.9, supporting the presence of five monosaccharide moieties in **1**. The presence of five methyl doublets at δ_H/δ_C 1.06/18.9, 1.12/18.7, 1.19/18.6, 1.17/18.5, and 1.06/19.0 suggested the presence of five deoxy sugar units in **1**. In addition, signals for methoxy groups of the sugar moieties were observed at δ_H/δ_C 3.33/59.6, 3.32/58.4, 3.29/56.5, 3.31/56.4, and 3.30/58.4, suggesting the 3-*O*-methylation of these deoxy sugars. The *β*-orientations of the anomeric centers were ascertained by the relatively large vicinal $^{3}J_{H\text{-}1,H\text{-}2(ax)}$ values of their corresponding anomeric protons (9.5–10.1 Hz) [13,26]. The existence of three *β*-D-cymaropyranosyl (Sug-1, 2, and 5) and two C-4 substituted *β*-D-oleandropyranosyl units (Sug-3 and 4) was confirmed by comparison of their carbon chemical shifts with those of the sugar moieties of reported steroidal glycosides [13,18,19,22,24]. The attachment of the sugar moieties to C-3 of the aglycone was deduced from HMBC cross peak between δ_H 4.75 (H-1 of Sug-1) and C-3 (δ_C 77.0) and confirmed by the downfield ^{13}C chemical shift of C-3 (δ_C 77.0). In the HMBC spectrum, correlations were observed between δ_H 4.69 (H-1 of Sug-2) and δ_C 82.2 (C-4 of Sug-1), δ_H 4.61 (H-1 of Sug-3) and δ_C 82.6 (C-4 of Sug-2), δ_H 4.55 (H-1 of Sug-4) and δ_C 82.4 (C-4 of Sug-3), and finally δ_H 4.77 (H-1 of Sug-5) and δ_C 82.3 (C-4 of Sug-4), establishing the sequence of the sugar moieties. Acid hydrolysis of **1** gave aglycone, cymarose, and oleandrose. The identification of monosaccharides and their absolute configurations

were confirmed by GCMS analysis of the hydrolysate and optical rotations measurement. The ^{1}H NMR and optical rotation measurements of aglycone confirmed it as 12-*O*-benzoylisolineolon. Inspection of the NMR spectral data (Tables 2 and 3) indicated that **1** had the same carbon skeleton as calotroposide A, which was previously isolated from *Calotropis gigantea* [15]. However, a difference in ^{13}C NMR chemical shift for C-17 was observed. The upfield shift of C-17 at δ_C 58.0 ppm in comparison to δ_C 60.3 ppm observed in calotroposide A, suggesting the epimerization of H-17 in **1**. Accordingly, **1** was identified as 12-*O*-benzoylisolineolon-3-*O*-*β*-D-cymaropyranosyl-(1 → 4)-*β*-D-cymaropyranosyl-(1 → 4)-*β*-D-oleandropyranosyl-(1 → 4)-*β*-D-oleandropyranosyl-(1 → 4)-*β*-D-cymaropyranosyl and generically named calotroposide H.

Compound **2** was isolated as brown viscous residue. The HRESIMS showed quasi-molecular ion peaks at *m/z* 1189.6524 $[M+H]^+$ and 1211.6338 $[M+Na]^+$, which was compatible with the molecular formula $C_{63}H_{96}O_{21}$ and thus identical to that of **1**. The IR, UV, and NMR spectral data of **2** (Tables 1–4) were also quite similar to those of **1** except the signals associated with the anomeric proton of the terminal D-cymarose at δ_H 4.77 (dd, *J* = 9.5, 2.4 Hz) and its carbon at δ_C 97.9 were absent in **2**. Instead, new signals at δ_H 4.47 (dd, *J* = 10.2, 2.1 Hz) correlated with the carbon signal at δ_C 100.8 in the HSQC experiment characteristic for the *β*-D-oleandrose moiety were observed. This indicated the terminal *β*-D-cymarose in **1** was replaced by *β*-D-oleandrose moiety in **2**. By comparison with the literature data together with those obtained from COSY, HSQC, and HMBC spectra, the structure of **2** was unambiguously elucidated as 12-*O*-benzoylisolineolon-3-*O*-*β*-D-cymaropyranosyl-(1 → 4)-*β*-D-cymaropyranosyl-(1 → 4)-*β*-D-oleandropyranosyl-(1 → 4)-*β*-D-oleandropyranosyl-(1 → 4)-*β*-D-oleandropyranosyl and named calotroposide I. The NMR data of **2** were basically identical to those found in calotroposide D previously reported from *C. gigantea* [20]. However, the $[\alpha]_D$ value of **2** was +18.1 (*c* 1.1, MeOH), while that of calotroposide D was −17.6 (*c* 1.1, $CHCl_3$), and C-17 was 1.7 ppm upfield shifted (δ_C 58.5) in comparison to that in calotroposide D (δ_C 60.2). These findings implied that **2** is a 17β-epimer of calotroposide D.

Compound **3** was obtained as brown viscous residue. The molecular formula was deduced as $C_{71}H_{108}O_{27}$ from HRESIMS quasi-molecular ion peak at *m/z* 1391.7005 $[M-H]^+$. Four prominent fragment ion peaks at *m/z* 1348.6 [(M−H)-43(acetyl group)]$^+$, 1186.4 [(M−H)-205 (acetyl Glu)]$^+$, 1081.8 [(M−H)-310 (acetyl Glu + benzoyl moiety)]$^+$, and 937.5 [(M−H)-454 (acetyl Glu + benzoyl moiety + Cym)]$^+$ were observed in the ESIMS spectrum. The IR spectrum showed absorption bands at 3480 (OH), 1710 (C=O), 1640, and 1055 cm^{-1}. The UV spectrum revealed absorption maxima at 230, 272, and 280 nm characteristic for the presence of benzoyl moiety. The NMR spectra exhibited signals characteristic of an oxypregnane oligoglycoside containing cymarose, oleandrose, and glucose moieties [16,21–23,25]. Comparison of the NMR data of **3** with those of **1** and **2** as well as the reported data for similar compounds supported the assignment of the aglycone of **3** as 12-*O*-benzoylisolineolon [13,17–20]. The ^{1}H and ^{13}C NMR spectra revealed the presence of six anomeric signals for six monosaccharide moieties at δ_H/δ_C 4.75 (dd, *J* = 9.5, 2.5 Hz)/95.0, 4.69 (dd, *J* = 9.5, 2.2 Hz)/99.3, 4.58 (dd, *J* = 10.1, 2.0 Hz)/99.3, δ_H 4.61 (dd, *J* = 10.2, 2.1 Hz)/100.6, 4.87 (dd, *J* = 9.5, 2.2 Hz)/96.9, and 4.18 (d, *J* = 7.2 Hz)/104.8. The presence of five methyl doublets at δ_H/δ_C 1.08/17.6, 1.10/17.9, 1.21/18.0, 1.18/18.1, and 1.12/17.8 suggested the presence of five deoxy sugar units in **3**. In addition, signals for methoxy groups of sugar moieties were observed at δ_H/δ_C 3.29/56.4, 3.30/56.4, 3.31/57.8, 3.32/57.6, and 3.33/59.0, suggesting the 3-*O*-methylation of these deoxy sugars. The *β*-orientations of the anomeric centers were ascertained by the relatively large $^3J_{H\text{-}1,H\text{-}2(ax)}$ values of their corresponding anomeric protons (7.2–10.2 Hz) [13,26]. The existence of a terminal *β*-D-glucopyranosyl unit (Sug-6), three C-4 substituted *β*-D-cymaropyranosyl (Sug-1, 2, and 5), and two C-4 substituted *β*-D-oleandropyranosyl units (Sug-3 and 4) was confirmed by comparison of their carbon chemical shifts with those of the sugar moieties of reported steroidal glycosides [13,16,17,19,20]. The attachment of the sugar moieties to C-3 of the aglycone was deduced from cross peak in HMBC experiment between δ_H 4.75 (H-1 of Sug-1) and C-3 (δ_C 76.3) and the downfield shift of C-3 (δ_C 76.3). The sequence of the sugar moieties was established by HMBC correlations between δ_H 4.69 (H-1 of Sug-2) and δ_C 81.9 (C-4 of Sug-1), δ_H 4.58 (H-1 of Sug-3) and δ_C 82.9 (C-4 of Sug-2), δ_H 4.61 (H-1 of Sug-4) and δ_C 82.2 (C-4 of Sug-3), δ_H 4.87 (H-1 of Sug-5) and δ_C 82.2 (C-4 of Sug-4), and δ_H 4.18 (H-1 of Sug-6) and δ_C 81.9 (C-4 of Sug-5). Furthermore, the NMR spectrum showed signals for an acetyl group at δ_H 1.98/δ_C 20.7 and 173.0, which was further confirmed by the fragment ion peak at *m/z* 1348.6 [(M−H)-43 (acetyl group)]$^+$ in the ESIMS spectrum. Its location was determined at C-6 of the terminal glucose unit (Sug-6) based on HMBC correlation of H_2-6 of glucose with the acetyl carbonyl at δ_C 173.0 and the downfield shift of C-6 of the 6-*O*-acetylated terminal glucose (δ_C 64.3) [27]. The monosaccharides of **3** and their absolute configurations were confirmed by acid hydrolysis followed by GCMS analysis of the hydrolysate and optical rotations measurement. From the above spectroscopic data, **3** was assigned as 12-*O*-benzoylisolineolon-3-*O*-*β*-D-cymaropyranosyl-(1 → 4)-*β*-D-cymaropyranosyl-(1 → 4)-*β*-D-oleandropyranosyl-(1 → 4)-*β*-D-oleandropyranosyl-(1 → 4)-*β*-D-cymaropyranosyl-(1 → 4)-(6-*O*-acetyl)-*β*-D-glucopyranoside and named calotroposide J.

Compound **4** was isolated as brown viscous residue. It gave a quasi-molecular ion peak at *m/z* 1349.6892 $[M-H]^+$ in the HRESIMS, consistent with a molecular formula $C_{69}H_{106}O_{26}$. Compound **4** is 42 mass units and one degree of unsaturation less than **3**. In addition, the ESIMS spectrum revealed three significant fragment ion peaks at *m/z* 1244.6 [(M−H)-105 (benzoyl group)]$^+$, 1081.6 [(M−H)-268 (benzoyl group + Glu)]$^+$, and 937.8 [(M−H)-412 (benzoyl moiety + Glu + Cym)]$^+$. The IR and UV spectra of **4** showed similar absorption patterns to those of **3**. The 1D and 2D NMR spectral data of **4** (Tables 1–4) were also quite similar to those of **3** except the absence of the signals associated with acetyl group at δ_H 1.98/δ_C 20.7 and 173.0 in **3**. On the basis of NMR and GCMS spectral data, **4** was assigned as 12-O-benzoylisolineolon-3-*O*-*β*-D-cymaropyranosyl-(1 → 4)-*β*-D-cymaropyranosyl-(1 → 4)-*β*-D-oleandropyranosyl-(1 → 4)-*β*-D-oleandropyranosyl-(1 → 4)-*β*-D-cymaropyranosyl-(1 → 4)-*β*-D-glucopyranoside and named calotroposide K.

Compound **5** was obtained as brown viscous residue. The molecular formula of **5** was established as $C_{68}H_{104}O_{28}$ based on the HRESIMS quasi-molecular ion peak at *m/z* 1367.6632 $[M-H]^+$. In addition, significant fragment ion peaks at *m/z* 1222.5 [(M−H)-145 (Ole)]$^+$, 1078.8 [(M−H)-289 (2 Ole)]$^+$, 934.6 [(M−H)-433 (2 Ole + Cym)]$^+$, 772.5 [(M−H)-595 (2 Ole + Cym + Glu)]$^+$, and 610.7 [(M−H)-757 (2 Ole + Cym + 2Glu)]$^+$ were observed in the ESIMS spectrum. By comparison of the 1D and 2D NMR spectra of **5** with those of **3** and **4**, the aglycone was identified as 12-*O*-benzoylisolineolon [13,17–19]. The ^{1}H NMR spectrum of **5** displayed six anomeric protons at δ_H 4.75 (dd, *J* = 9.5, 2.2 Hz, H-1 of Cym-1), 4.40 (d, *J* = 7.6 Hz, H-1 of Glu-2), 4.28 (d, *J* = 7.2 Hz, H-1 of Glu-3), 4.69 (dd, *J* = 9.5, 2.4 Hz, H-1 of Cym-4), 4.61 (dd, *J* = 10.2, 2.0 Hz, H-1 of Ole-5), and 4.56 (dd, *J* = 10.2, 2.0 Hz, H-1 of Ole-6) (Tables 3 and 4). These anomeric protons were correlated to their corresponding carbons at δ_C 95.3 (C-1 of Cym-1), 103.0 (C-1 of Glu-2), 103.6 (C-1 of Glu-3), 99.7 (C-1 of Cym-4), 99.6 (C-1 of Ole-5), and 100.9 (C-1 of Ole-6), respectively in the multiplicity-edited HSQC spectrum. Comparison of the carbon chemical shifts with those reported in the literature indicated that **5** contains two 4-substituted *β*-D-cymaropyranosyl, two 4-substituted

β-D-oleandropyranosyl, and two 4-substituted β-D-glucopyranosyl units [13,16–19,21,22]. The β-orientations of the anomeric protons of these monosaccharides were supported by the relatively large vicinal coupling constant $^{3}J_{H\text{-}1,H\text{-}2ax}$ values of their anomeric protons (7.2–10.2 Hz). As previously described, the HMBC correlations allowed the establishment of the sugar sequence in **3**. Similarly, the HMBC spectrum of **5** displayed cross peaks between δ_H 4.75 (H-1 of Cym-1) and C-3 of aglycone (δ_C 76.9), δ_H 4.40 (H-1 of Glu-2) and δ_C 82.1 (C-4 of Cym-1), δ_H 4.28 (H-1 of Glu-3) and δ_C 80.7 (C-4 of Glu-2), δ_H 4.69 (H-1 of Cym-4) and δ_C 80.6 (C-4 of Glu-3), δ_H 4.61 (H-1 of Ole-5) and δ_C 82.2 (C-4 of Cym-4), and finally between δ_H 4.56 (H-1 of Ole-6) and δ_C 82.3 (C-4 of Ole-5). Thus, the sequence of the sugar moieties had been concluded to be β-D-cymaropyranosyl-(1 → 4)-β-D-glucopyranosyl-(1 → 4)-β-D-glucopyranosyl-(1 → 4)-β-D-cymaropyranosyl-(1 → 4)-β-D-oleandropyranosyl-(1 → 4)-β-D-oleandropyranoside and further confirmed by the ESIMS fragmentation pattern. From the above discussion, **5** was identified as 12-*O*-benzoylisolineolon-3-*O*-β-D-cymaropyranosyl-(1 → 4)-β-D-glucopyranosyl-(1 → 4)-β-D-glucopyranosyl-(1 → 4)-β-D-cymaropyranosyl-(1 → 4)-β-D-oleandropyranosyl-(1 → 4)-β-D-oleandropyranoside and named calotroposide L.

Compound **6** was isolated as brown viscous residue. The molecular formula was deduced to be $C_{78}H_{120}O_{30}$ based on HRESIMS quasi-molecular ion peak at *m/z* 1537.7941 $[M+H]^+$, being two sugar moieties larger than calotroposide I (**2**). It showed significant fragment ion peaks at *m/z* 1494.6 $[(M+H)\text{-}43\ (COCH_3)]^+$, 1332.7 $[(M+H)\text{-}205\ (\text{acetyl} + \text{Glu})]^+$, 1188.8 $[(M+H)\text{-}349\ (COCH_3 + \text{Glu} + \text{Ole})]^+$, and 1044.6 $[(M+H)\text{-}493\ (COCH_3 + \text{Glu} + 2\ \text{Ole})]^+$ in the ESIMS spectrum. The aglycone moiety of **6** was identified as 12-*O*-benzoylisolineolon by comparison of its NMR spectral data with those of **1–5** and values in the literature (Tables 1 and 2) [13,17–20]. The ^{1}H and ^{13}C NMR spectroscopic data of **6** were similar to those of calotroposide I (**2**) together with additional signals for two anomeric protons at δ_H 4.38 (dd, *J* = 10.1, 2.5 Hz, H-1 of Ole-6) and 4.26 (d, *J* = 7.8 Hz, H-1 of Glu-7), correlated with the carbon signals at δ_C 102.6 and 103.1, respectively in the multiplicity-edited HSQC spectrum suggesting the presence of additional glucose and oleandrose moieties. This was further confirmed by comparison of the ^{1}H and ^{13}C NMR chemical shifts with literature as well as the ESIMS fragment ion peaks at 1332.7 $[(M+H)\text{-}205\ (\text{acetyl} + \text{Glu})]^+$ and 1188.8 $[(M+H)\text{-}349\ (COCH_3 + \text{Glu} + \text{Ole})]^+$. Moreover, signals at δ_H 1.91/δ_C 21.0 and 173.0 indicated the presence of an acetyl group in **6**. This was confirmed by the fragment ion peak at *m/z* 1494.6 $[(M+H)\text{-}43\ (\text{acetyl})]^+$ in the ESIMS spectrum. Its location at C-6 of the terminal glucose moiety was established from HMBC correlation from H_2-6 of glucose to the carbonyl group of the acetyl moiety at δ_C 173.0 and supported by the downfield shift of C-6 of the terminal 6-*O*-acetylated glucose (δ_C 63.9) [27]. A detailed analysis of 1D and 2D NMR spectral data as well as mass fragmentation pattern revealed that the sugar part of **6** consists of two β-D-cymaropyranoses, four β-D-oleandropyranoses, and one 6-acetyl-β-D-glucopyranose [13,16–19,21,22]. Again, the aglycone moiety of **6** was identified as 12-*O*-benzoylisolineolon. Finally, after acid hydrolysis of **6**, the optical rotation as well as GCMS of the purified monomeric sugars were measured and compared with the previously reported values showing that the sugar moieties possess a β-D-configuration. The HMBC correlations unambiguously established the sequence and connectivity of the sugar moieties. From the above mentioned data, **6** was assigned as 12-*O*-benzoylisolineolon-3-*O*-β-D-cymaropyranosyl-(1 → 4)-β-D-cymaropyranosyl-(1 → 4)-β-D-oleandropyranosyl-(1 → 4)-β-D-oleandropyranosyl-(1 → 4)-β-D-oleandropyranosyl-(1 → 4)-β-D-oleandropyranoside-(1 → 4)-(6-*O*-acetyl)-β-D-glucopyranoside and named calotroposide M.

Compound **7** was obtained as brown viscous residue. On the basis of HRESIMS quasi-molecular ion peak at *m/z* 1511.7418 $[M-H]^+$, the molecular formula of **7** was determined to be $C_{75}H_{116}O_{31}$, which was 324 mass units more than calotroposide I (**2**), indicating the presence of two additional glucose units in **7**. This was established by the appearance of two anomeric proton signals at δ_H 4.27 (d, *J* = 7.8 Hz) and 4.40 (d, *J* = 7.8 Hz), correlated with the carbon signals at δ_C 103.1 and 102.6, respectively in the multiplicity-edited HSQC spectrum. This was further confirmed by ESIMS fragment ion peaks at *m/z* 1349.6 $[(M-H)\text{-}162\ (\text{Glu})]^+$ and 1186.3 $[(M-H)\text{-}325\ (2\text{Glu})]^+$. The connectivity of the two glucose units was 1 → 4 based on the HMBC correlations. All the glycosidic linkages have β-D-configurations as judged from the coupling constant values and acid hydrolysis of **7**, followed by GCMS analysis and optical rotations determination of the resulted sugars. The aglycone of **7** was identified as 12-*O*-benzoylisolineolon by comparison of the NMR spectral data with compounds **1–6** and reported data in literature (Tables 1 and 2) [13,17–20]. By the HSQC, HMBC, and COSY correlations, all the carbons of the sugar moieties were assigned to their proton signals. The seven sugar units of **7** were identified as two β-D-cymaropyranoses, three β-D-oleandropyranoses, and two β-D-glucopyranoses. By comparison of the NMR data with literature, as well as the observed HMBC correlations, the sequence and linkage sites of the sugar units were established as β-D-cymaropyranosyl-(1 → 4)-β-D-cymaropyranosyl-(1 → 4)-β-D-oleandropyranosyl-(1 → 4)-β-D-oleandropyranosyl-(1 → 4)-β-D-oleandropyranosyl-(1 → 4)-β-D-glucopyranoside-(1 → 4)-β-D-gluopyranoside. On the basis of the above evidences, **7** was assigned as 12-*O*-benzoylisolineolon-3-*O*-β-D-cymaropyranosyl-(1 → 4)-β-D-cymaropyranosyl-(1 → 4)-β-D-oleandropyranosyl-(1 → 4)-β-D-oleandropyranosyl-(1 → 4)-β-D-oleandropyranosyl-(1 → 4)-β-D-glucopyranoside-(1 → 4)-β-D-gluopyranoside and named calotroposide N.

Compounds **1–7** were evaluated for their *in vitro* growth inhibitory activity against A549 NSCLC, U373 GBM, and PC-3 prostate cancer cell lines using the MTT colorimetric assay. The most active compounds included compounds **4** and **6**. Both compounds exhibited one magnitude of difference in terms of growth inhibitory activity among the tested three cancer cell lines (Table 5). The less active compounds included **3**, **5**, and **7**, while compounds **1** and **2** were moderately active.

Since compounds **1–7** possess the same aglycone moiety (12-*O*-benzoylisolineolon) and according to the data presented in Table 5, it could be concluded that neither the number of sugar residues attached to alcoholic moiety at C-3 of the aglycone moiety (compound **1** versus **2**; compound **4** versus **3** and **5**; and compound **6** versus **7**) nor the sequence of the sugar residues on the side chain have direct effect on the activity of the compounds. In addition, 6-*O*-acetylation of the terminal glucose residue in the highly active **4** resulted in decrease of the activity by 13–50 folds as observed in **3**, suggesting the importance of the acetyl moiety in this side chain. On the contrary and despite their difference in one sugar residue,

Table 5
In vitro growth inhibitory activity results.

Compound	IC_{50} (μM)			
	A549 NSCLC	U373 GBM	PC-3 prostate cancer	Mean ± SEM
n-BuOH[a]	0.2	0.5	1.0	0.5 ± 0.2
1	3.3	21.8	17.6	14.0 ± 7
2	23.5	3.3	4.2	10.0 ± 8
3	61.7	32.3	34.4	43.0 ± 13
4	4.4	0.5	0.7	1.8 ± 1
5	72.3	14.6	39.4	42.0 ± 23
6	4.5	0.5	0.6	1.8 ± 2
7	66.0	24.4	44.9	45.0 ± 24

[a] The growth inhibitory effects of the *n*-BuOH fraction are expressed as μg/mL.

6-*O*-acetylation of the terminal glucose unit of **6** shows increase in the activity by 15–75 folds in comparison to **7**. Despite, **1** and **2** possess the same number of sugar residues with only difference in the terminal sugar residue. They display variable selectivity towards the three cancer cells lines (Table 5).

The differences in terms of *in vitro* growth inhibitory activity between compounds **4** and **6** on the one part, and on the other, between compounds **3**, **5** and **1**, **2**, and **7** could reflect distinct binding affinities of these compounds for the alpha-1 subunit of the sodium pump, which is a receptor for cardiotonic steroids and which is variably expressed in cancer cells as previously showed for other types of cardiotonic steroids [28].

4. Conclusion

Seven new oxypregnane oligoglycosides; calotroposides H–N (**1–7**) were isolated from root barks of *C. procera*. The structures of these compounds were established on the basis of their spectroscopic data. Compounds **4** and **6** showed growth inhibition activity against U373 glioblastoma (GBM) and PC-3 prostate cancer cell lines.

Acknowledgments

We would like to express our deep thanks to Mr. Volker Brecht (Institut für Pharmazeutische Wissenschaften, Albert-Ludwigs Universität, Freiburg, Germany) for acquiring NMR and MS spectroscopic data.

References

[1] Doshi H, Satodiya H, Thakur MC, Parabia F, Khan A. Phytochemical screening and biological activity of *Calotropis Procera* (Ait). R. Br. (Asclepiadaceae) against selected bacteria and *Anopheles stephansi* larvae. Int J Plant Res 2011;1:29–33.
[2] Tour N, Talele G. Anti-inflammatory and gastromucosal protective effects of *Calotropis procera* (Asclepiadaceae) stem bark. J Nat Med 2011;65:598–605.
[3] Ibrahim MA, Aliyu AB, Meduteni K, Yunusa I. Saponins-rich fraction of *Calotropis procera* leaves elicit no antitrypanosomal activity in a rat model. Asian Pac J Trop Biomed 2013;3:569–72.
[4] Iqbal Z, Lateef M, Muhammad AG, Khan MN. Anthelmintic activity of *Calotropis procera* (Ait). flowers in sheep. J Ethnopharmacol 2005;102:256–61.
[5] Iwalewa EO, Elujoba AA, Bankole OA. *In vitro* spasmolytic effect of aqueous extract of *Calotropis procera* on guinea-pig trachea smooth muscle chain. Fitoterapia 2005;76:250–3.
[6] Van Quaquebeke E, Simon G, André A, Dewelle J, El Yazidi M, Bruyneel F, et al. Identification of a novel cardenolide (2-oxovoruscharin) from *Calotropis procera* and the hemisynthesis of novel derivatives displaying potent *in vitro* antitumor activities and high *in vivo* tolerance: structure–activity relationship analyses. J Med Chem 2005;48:849–56.
[7] Yesmin MN, Uddin SN, Mubassara S, Akond MA. Antioxidant and antibacterial activities of *Calotropis procera* Linn.. American-Eurasian J Agric Environ Sci 2008;4:550–3.
[8] Bharti S, Wahane VD, Kumar VL. Protective effect of *Calotropis procera* latex extracts on experimentally induced gastric ulcers in rat. J Ethnopharmacol 2010;127:440–4.
[9] Moustafa AM, Ahmed SH, Nabil ZI, Hussein AA, Omran MA. Extraction and phytochemical investigation of *Calotropis procera*: effect of plant extracts on the activity of diverse muscles. Pharm Biol 2010;48:1080–190.
[10] Sharma A, Rathore GS, Sharma MS, Choudhary V, Kumar B, Bhandari A. Pharmacological evaluation of stem of *Calotropis procera* for hepatoprotective activity. Int J Res Pharm Chem 2011;1:143–7.
[11] Ibrahim SRM, Mohamed GA, Shaala LA, Banuls LM, Van Goietsenoven G, Kiss R, et al. New ursane-type triterpenes from the root bark of *Calotropis procera*. Phytochem Lett 2012;5:490–5.
[12] Ibrahim SRM, Mohamed GA, Shaala LA, Banuls LM, Van Goietsenoven G, Kiss R, et al. A new cardiac glycoside from the root barks of *Calotropis procera* with in vitro anticancer effects. Nat Prod Res 2014;28:1322–7.
[13] Kuroda MI, Kubo S, Uchida S, Sakagami H, Mimaki Y, Amurensiosides A-K. 11 new pregnane glycosides from the roots of *Adonis amurensis*. Steroids 2010;75:83–94.
[14] Abdallah HM, Osman AM, Almehdar H, Abdel-Sattar E. Acylated pregnane glycosides from *Caralluma quadrangula*. Phytochemistry 2013;88:54–60.
[15] Li XY, Sun HX, Ye YP, Chen FY, Pan YJ. C-21 steroidal glycosides from the roots of *Cynanchum chekiangense* and their immunosuppressive activities. Steroids 2006;71:61–6.
[16] Kitagawa I, Zhang R, Park JD, Baek NI, Takeda Y, Yoshikawa M, et al. Indonesian medicinal plants. I. Chemical structures of calotroposides A and B, two new oxypregnane-oligoglycosides from the root of *Calotropis gigantea* (Asclepiadaceae). Chem Pharm Bull 1992;40:2007–13.
[17] Kimura M, Hayashi K, Narita H, Mitsuhashi H. Studies on the constituents of Asclepiadaceae plants. Li. Oxidation at the 18-methyl group of C/D-cis-pregnane type steroids and ^{13}C-nuclear magnetic resonance spectra of 18-oxygenated pregnanes and related compounds. Chem Pharm Bull 1982;30:3932–41.
[18] Warashina T, Noro T. Cardenolide and oxypregnane glycosides from the root of *Asclepias incarnata* L.. Chem Pharm Bull 2000;48:516–24.
[19] Warashina T, Noro T. Acylated-oxypregnane glycosides from the roots of *Araujia sericifera*. Chem Pharm Bull 2003;51:1036–45.
[20] García VP. Acid epimerization of 20-keto pregnane glycosides is determined by 2D-NMR spectroscopy. J Biomol NMR 2011;50:91–7.
[21] Shibuya H, Zhang R, Park JD, Baek NI, Takeda Y, Yoshikawa M, et al. Indonesian medicinal plants. V. Chemical structures of calotroposides C, D, E, F, and G, five additional new oxypregnane-oligoglycosides from the root of *Calotropis gigantea* (Asclepiadaceae). Chem Pharm Bull 1992;40:2647–53.
[22] Abe F, More Y, Okabe H, Yamauchi T. Steroidal constituents from the roots and stems of *Aclepias fruticosa*. Chem Pharm Bull 1994;42:1777–83.
[23] Warashina T, Noro T. Acylated-oxypregnane glycosides from the roots of *Asclepias syriaca*. Chem Pharm Bull 2009;57:177–84.
[24] Abe F, Yamauchi T. Pregnane glycosides from the roots of *Asclepias tuberosa*. Chem Pharm Bull 2000;48:1017–22.
[25] Li J, Liu H, Lin Y, Hao X, Ni W, Chen C. Six new C21 steroidal glycosides from *Asclepias curassavica* L. Steroids 2008;73:594–600.
[26] Agrawal PK. NMR spectroscopy in the structural elucidation of oligosaccharides and glycosides. Phytochemistry 1992;31:3307–30.
[27] Kim SY, Gao JJ, Lee W-C, Ryu KS, Lee KR, Kim YC. Antioxidative flavonoids from the leaves of *Morus alba*. Arch Pharm Res 1999;22:81–5.
[28] Banuls LMY, Katz A, Miklos W, Cimmino A, Tal DM, Ainbinder E, et al. Hellebrin and its aglycone form hellebrigenin display similar *in vitro* growth inhibitory effects in cancer cells and binding profiles to the alpha subunits of the Na^+/K^+-ATPase. Mol Cancer 2013;12:1–14. https://www.researchgate.net/publication/236457162_Hellebrin_and_its_aglycone_form_hellebrigenin_display_similar_in_vitro_growth_inhibitory_effects_in_cancer_cells_and_binding_profiles_to_the_alpha_subunits_of_the_NaK-ATPase?ev=prf_pub.